Environmental Pollution 334 (2023) 122147

Contents lists available at ScienceDirect

Environmental Pollution

journal homepage: www.elsevier.com/locate/envpol

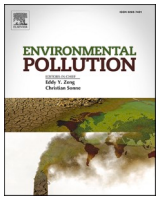

Changes in air dose rates due to soil moisture content in the Fukushima prefecture forests☆

Miyu Nakanishi [a], Yuichi Onda [b,*], Junko Takahashi [b], Hiroaki Kato [b], Hikaru Iida [a], Momo Takada [c]

[a] University of Tsukuba, Tsukuba, Ibaraki, 305-8572, Japan
[b] Center for Research in Isotopes and Environmental Dynamics, University of Tsukuba, Tsukuba, Ibaraki, 305-8572, Japan
[c] National Institute of Advanced Industrial Science and Technology, Tsukuba, Ibaraki, 305-8567, Japan

ARTICLE INFO

Keywords:
Air dose rate
Soil moisture content
Effective rainfall
Shielding effect
Hysteresis

ABSTRACT

Radionuclides released and deposited because of the 2011 Fukushima Dai-ichi Nuclear Power Plant accident caused an increase in air dose rates in Fukushima Prefecture forests. Although an increase in air dose rates during rainfall was previously reported, the air dose rates in the Fukushima forests decreased during rainfall. This study aimed to develop a method to estimate rainfall-related changes in air dose rates, even in the absence of soil moisture data, in Namie-Town and Kawauchi-Village, Futaba-gun, Fukushima Prefecture. Moreover, we examined the relationship between preceding rainfall (*Rw*) and soil moisture content. The air dose rate was estimated by calculating the *Rw* in Namie-Town from May to July 2020. We found that the air dose rates decreased with increasing soil moisture content. The soil moisture content was estimated from *Rw* by combining short-term and long-term effective rainfall using half-live values of 2 h and 7 d and considering the hysteresis of water absorption and drainage processes. Furthermore, the soil moisture content and air dose rate estimations showed a good agreement with coefficient of determination (R^2) scores >0.70 and >0.65, respectively. The same method was tested to estimate the air dose rates in Kawauchi-Village from May to July 2019. At the Kawauchi site, variation in estimated value is relatively large due to the presence of water repellency in dry conditions, and the amount of ^{137}Cs inventory was low, so estimating air dose from rainfall remained a challenge. In conclusion, rainfall data were successfully used to estimate soil moisture and air dose rates in areas with high ^{137}Cs inventories. This leads to the possibility of removing the influence of rainfall on measured air dose rate data and could contribute to the improvement of methods currently used to estimate the external air dose rates for humans, animals, and terrestrial forest plants.

1. Introduction

Air dose rate is often used to measure the radiation dose of a particular environmental site. The Fukushima Dai-ichi Nuclear Power Plant accident in March 2011 has resulted in the release of radioactive cesium into the atmosphere, and the distribution of ^{137}Cs and naturally occurring radionuclides in the Fukushima forests. Following the FDNPP accident, 2.7 PBq of ^{137}Cs was deposited onto the terrestrial environment, 67% of which fell out onto forests (Onda et al., 2020). In the forests, the initial deposited ^{137}Cs migrated from the canopy and trunks to the forest floor over time by the falling of leaves, branches, and rain, as well as through three types of radioactive migration that occur in forests, namely new defoliation, the movement of topsoil and other materials, and movement from the litter layer to deeper soil. These transfers change the radiation sources in forests over time (Kato et al., 2018).

The radioactive cesium deposited in these forests emits high-energy γ-rays owing to the decay of its nucleus, which increases the radiation dose (Basuki et al., 2020). Radiation levels are mainly influenced by radioactive materials that have been deposited in the tree canopy and those that have migrated to the ground surface and deeper into the soil. Since 2017, the highest radiation levels were detected within 5 cm from the soil surface. This could be attributed to the presence of radioactive cesium in the soil surface layer (Malins et al., 2021).

☆ This paper has been recommended for acceptance by Hefa Cheng.

* Corresponding author. University of Tsukuba, 1Tennoudai, Tsukuba, Ibaraki, 305-8572, Japan.
E-mail addresses: na73mi26@gmail.com (M. Nakanishi), onda@geoenv.tsukuba.ac.jp (Y. Onda).

https://doi.org/10.1016/j.envpol.2023.122147
Received 6 February 2023; Received in revised form 19 June 2023; Accepted 3 July 2023
Available online 8 July 2023

Temporal changes in air dose rates are caused by the effects of wind, rainfall, and snowfall. The variation in natural radiation on rainfall-free and snowfall-free days is mainly governed by changes in soil aridity and the concentrations of radon daughter radionuclides in the atmosphere (Minato, 1980). During snowfall, the air dose rate decreases (Nagaoka et al., 1988) owing to shielding of the radiation dose rate from the ground. During rainfall, the air dose rate increases owing to the contribution of the decay products of wet-deposited ^{222}Rn (Tsuchida et al., 2020). In contrast, when rainfall saturates the soil, the air dose rates decreases compared to that in dry conditions (Schimmack et al., 1998). In the Fukushima Prefecture forests, air dose rates are known to temporarily decrease during rainfall (Imamura et al., 2017). Soil moisture is a crucial factor in determining dose rates because it affects soil bulk density and attenuates the effective exposure to nuclear radiation (Nelson and Rittenour, 2015). In the Fukushima Prefecture forests, the effect of radionuclide shielding on the ground surface by moisture in the soil is considered more significant than the increase in air dose rates due to natural radionuclide fallout during rainfall. Therefore, it is necessary to understand changes in air dose rates due to rainfall and changes in soil moisture content to assess the air dose rate in the Fukushima forests.

Soil moisture data can provide a direct indication of the radiation-shielding effect of the wet and dry conditions of the soil and litter layers. Although soil moisture content can be measured in the field using soil moisture sensors, it is costly and labor intensive, and only indicates data for that specific location. In the absence of soil moisture data, information on soil moisture can be obtained from the antecedent rainfall index (API) and the effective rainfall (*Rw*). The effective rainfall or leading rainfall index is calculated by decreasing the effect of past rainfall over time. The *Rw* has a good correlation with the hydraulic head pressure in the soil (Shimamura, 2003), and there is a high correlation between the *Rw* values obtained from daily continuous rainfall data and changes in soil moisture content (Fukuda et al., 2009). Therefore, if the *Rw* can be calculated using hourly rainfall data and the moisture status of the soil can be estimated, it will be possible to easily evaluate changes in the air dose rate.

Regarding soil moisture dynamics, water gradually percolates from small to large pore spaces during the water absorption process. However, in the drainage process, water is more likely to accumulate in fine pore spaces than in coarse pore spaces. This results in hysteresis, in which the water absorption and drainage processes do not follow the same path. Water repellency was observed in approximately 92% of soils in temperate ecosystems (Seaton et al., 2019) as well as in Japanese forest soil (Kobayashi, 2013). Water-repellent surface soils resist infiltration. Moreover, soil water repellency is rarely uniform (Cammeraat and Imeson, 1999; Keizer et al., 2008; Lozano et al., 2013; Urbanek et al., 2015), and is often characterized by very uneven and heterogeneous wetting patterns (Smettem et al., 2021). To accurately describe the hydraulic behavior of soil water, it is necessary to consider hysteresis and the water repellency effect (Mirbabaei et al., 2021). Therefore, *Rw* estimated from preceding rainfall may be preferable to soil moisture content data, which is a local dataset. None of the previous studies considered soil water infiltration properties when comparing soil moisture content and air dose rate. The relationship between rainfall and soil moisture content and their effect on air dose can be revealed through field measurements.

Therefore, we estimated changes in air dose rates based on changes in soil moisture content in two target areas in the Fukushima Prefecture forests. Furthermore, we used rainfall data to determine the soil moisture status due to effective rainfall and estimate changes in air dose rates.

2. Material and methods

2.1. Study site

A forested watershed located in the Akougi district of Namie-Town, Futaba-gun, Fukushima Prefecture, was selected as the first target area (Fig. 1). The watershed area was 7749 m^2, the average annual precipitation from 2010 to 2019 was 1442 mm (Tsushima Station, Japan Meteorological Agency (JMA)), and the average annual temperature is 10.5 °C (Iidate Station, JMA). This area is located approximately 23 km northwest of the Fukushima Dai-ichi Nuclear Power Plant and, as of 2022, is still designated as a difficult-to-return zone because of the large amount of deposited radioactive materials. As of July 2, 2011, the initial deposition of radioactive materials released during the FDNPP accident was 4727 kBq/m^2. The tree species in the forest mainly comprise conifers, such as Japanese cedar (*Cryptomeria japonica*) and red pine, and broad-leaved trees, such as *Quercus Serrata*, chestnut, maples, and Japanese maples. Our observations were conducted in plots constructed in young cedar forests in the target watershed area. In the target cedar forest area, the density of standing trees was 3300 trees/ha, the average tree height was 18 m, and the average canopy openness was 31.5%. At the 0–10 cm surface layer, the vapor phase in the three-phase distribution of the soil was 60%, and wet throughout the year.

The second target area was a cedar forest in the Kawauchi Experimental Forest of the Fukushima Forestry Research Center, located in Nabekura, Shimokawauchi, Kawauchi-Village, Futaba-gun, Fukushima Prefecture. This area has been the site of a long-term monitoring survey conducted by the Forestry Agency since 2012, after the Fukushima Dai-ichi Nuclear Power Plant accident. As of 2012, the forest was a 43-year-old cedar forest with an average slope of 34°. In November 2012, the average deposition of radioactive cesium was 1120 kBq/m^2, with an air dose rate of 2.2–4.5 μSv/h. Since the start of observations in the study area, the air dose rate at this site has continued to decrease; by 2019, it had decreased by approximately 50%, and the current air dose rate is approximately 0.30 μSv/h. As of 2019, the cedar forest was 7 years old, and the height of the trees was approximately 2–3 m. The vapor phase in the three-phase distribution of the soil was 43%, and the soil had a high porosity. The background absorbed dose rates in the areas shown in Fig. 1 range of 0.0045–0.09 μGy/h (Sanada et al., 2020).

2.2. Field sampling

To confirm the effects of rainfall on the variation in air dose rates, observations using simple, continuous, and recordable instruments were conducted as follows.

In the Namie-Town target area, observations were conducted for 63 days, from May 14 to July 15, 2021. These were periods of small fluctuations in air dose rates in the forest owing to the effects of less falling leaves. A survey plot of approximately 3 × 3 m was created within the site, six soil moisture content sensors (S-SMD-005; Oneset) were installed at a depth of 5 cm, and soil moisture was measured at hourly intervals. Five D-Shuttle dosimeters (Chiyoda Technol, Inc.), which record data for approximately one year, were placed at a height of 1 m in the four corners and center of the survey plot. The dosimeters were wrapped in plastic bags with waterproof zippers. The measurement range of the D-Shuttle is 0.1 μSv/h to 99.99 mSv/h, and their minimum detection value of 0.01 μSv/h. The count values are recorded for each period (total accumulation, monthly accumulation, daily accumulation, and hourly accumulation), and the dose is calculated by multiplying by a calibration constant. The value is expressed in terms of the ambient dose equivalent H*(10). Kawano et al. (2019) compared D-Shuttle and NaI (Tl) scintillation survey meters, with a daily coefficient of variation of 7.19%. Adachi et al. (2016) used them in wide-area surveys in low-dose areas in Japan, France, Poland, etc. On May 6, June 10, and July 12, 2021, the air dose rates were also measured using NaI (Tl) scintillation survey meters (TCS-172B; Hitachi Aloka Medical) to confirm whether there were differences to the measured values obtained from D-Shuttle dosimeters.

For the survey in the Kawauchi-Village, the observations were conducted in the same season as that in Namie-Town for 72 days, from May 6 to July 16, 2019. To determine the soil moisture content, an ADR soil

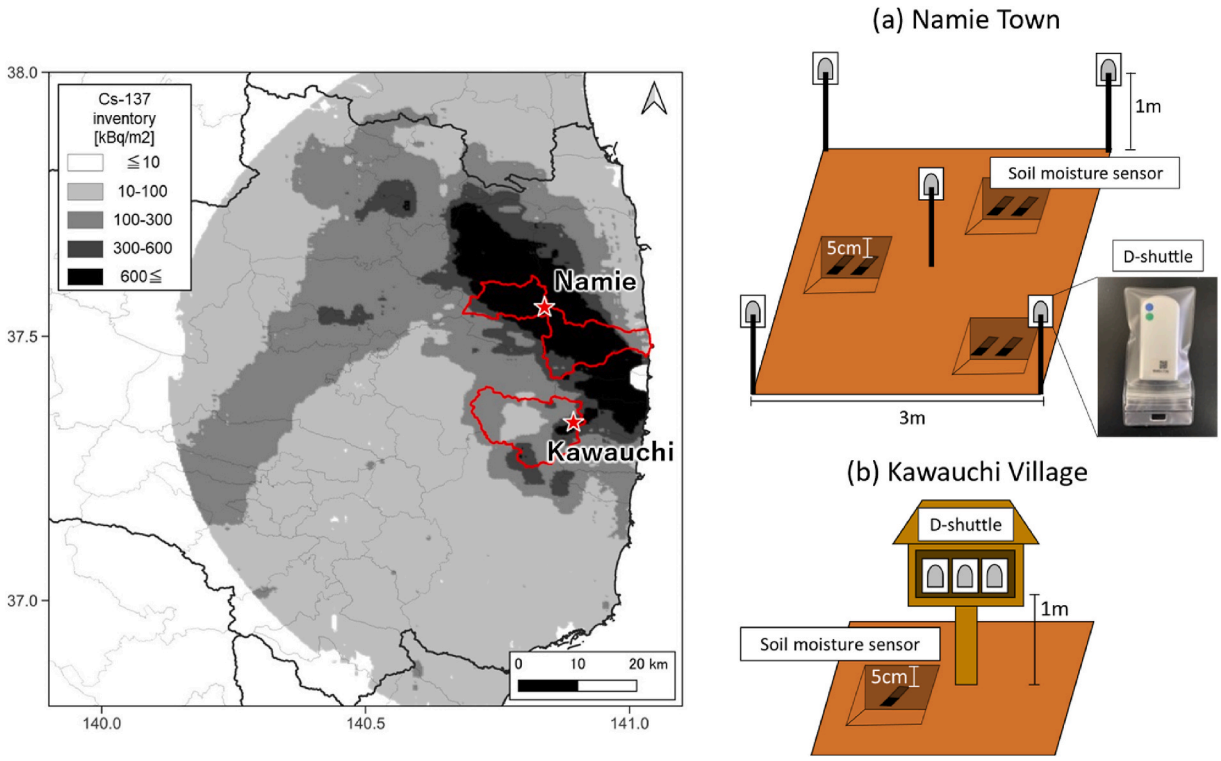

Fig. 1. Study site and method.

moisture meter (UIR-SM-2X; Uijin) was used; the sensor was buried in the soil at a depth of approximately 5 cm, and the volumetric moisture content was measured and recorded every 10 min. In addition, air dose rates were continuously observed in March 2019 using a D-Shuttle dosimeter (Chiyoda Technol, Inc.). Three dosimeters wrapped in food wrap film or plastic bags with zippers for waterproofing were installed at one location in a storage box at a height of approximately 1 m. In addition, the air dose rates were measured on May 17 and June 14, 2019 using an NaI (Tl) scintillation survey meter (TCS-172B; Hitachi Aloka Medical).

2.3. Air dose rate estimation using the soil moisture content

The relationship between soil moisture content and air dose rate was examined to determine whether the rainfall-related reduction in air dose rate affects the soil moisture content. Since the air dose rates in forests are determined by the distribution of radioactive materials, such as the presence of deposited radioactive materials in trees and fallen leaves as well as the total amount of radioactive materials in the soil layer, and atmospheric disturbances, such as strong winds and rainfall, causes temporary changes in air dose rates. Therefore, to reduce the influence of hourly data variations in the air dose rates, a value $z_{(t)}$ (Eq. (1)) was used, which is the average of $Z_{(t)}$ at time t, $Z_{(t-1)}$ at time *t-1* 1 h earlier, $Z_{(t-2)}$ at time *t-2* 2 h earlier, $Z_{(t+1)}$ at time *t+1* 1 h later, and $Z_{(t+2)}$ at time *t+2* 2 h later.

$$z_{(t)} = \frac{1}{5}\sum_{-2}^{2} Z_{(t-i)} \tag{1}$$

This allowed us to capture rainfall-related changes in air dose rates that lasted for several hours and to eliminate the effects of changes in air dose rates due to temporary atmospheric disturbances. Similarly, a moving average was used to determine the soil moisture content. The results are shown in Supplementary Fig. 1.

In this paper, the main results from Namie-Town as the basis for this paper, and the data from Kawauchi-Village are used as a comparative example. The observed trends of soil moisture content and air dose rate in Namie-Town were quite similar (the average correlation coefficient of soil moisture content by location was *r=0.92*, and the average correlation coefficient of air dose rate was *r=0.79*). Therefore, the number of measuring instruments used has not quite significant impact on the results. On the other hand, a large number of data is certainly more reliable, and the reproducibility of the values for the Kawauchi site may be low due to the small number of soil moisture sensors in use. As for the air dose rate, there were no significant differences compared to the same location in Kawauchi-Village, because it exhibited almost the same fluctuation trend even though the sensors were installed up to 4 m apart in Namie-Town.

2.4. Soil moisture content and air dose rate estimation using effective rainfall

To analyze changes in soil moisture content and air dose rate over time, the effective rainfall (*Rw*) was calculated using hourly rainfall data recorded at the Tsushima station and compared with the measured soil moisture content and air dose rate. *Rw* is expressed in Eq. (2):

$$Rw = \sum_{0}^{n} \alpha^{i} R_i \tag{2}$$

where R_0 is the current hourly rainfall [mm/h], R_n is the hourly rainfall *n* h ago [mm/h], *T*: half-life [h]. Here, *n=720* was used to consider the effect of preceding rainfall for *T* over the past 30 days.

The *Rw* value changes by changing *T* in Eq. (3):

$$\alpha = (0.5)^{\frac{1}{T}} \tag{3}$$

Based on the data obtained from the soil moisture content observations, we calculated *Rw* to determine the soil moisture status. For this purpose, it is necessary to determine *Rw* using an optimal *T* that correlates well with soil moisture content. Here, 33 different *Rw* were calculated using *T* values from 1 to 24 h and then up to 240 h (10 days) at 24-h intervals. The *T* value that had the best relationship with the soil

moisture content was selected. The *Rw* value, using the half-lives calculated above, was compared with the soil moisture content, and the air dose rate was estimated from the *Rw* value at that time.

2.5. Water repellency strength

The intensity of water repellency at the study site was measured. 100 mL of 0–5 cm soil samples were collected, transported to the laboratory, dried, and sieved through a 2 mm sieve. The soil samples were rewetted to prepare soils with various moisture contents. In total, 31 different concentrations of ethanol solution (0.1 mL), ranging from 0 to 30% in 1% increments, were gently dropped onto the soil samples. The ethanol concentration (ethanol fraction [EP]) was then measured when all had penetrated after 5 s. If a 0% ethanol solution penetrated within 5 s, the measured value was uniformly set to 0.

3. Results of Namie site

3.1. Temporal changes during the observation period

Information on observed rainfall, soil moisture content, and air dose is shown in Table 1. Rainfall occurred regularly during the observation period, with a total accumulation of 313 mm and maximum hourly rainfall of 17.5 mm. Soil moisture content ranged from 28% to 37% throughout the observation period. Air dose rates varied between 5.23 and 6.87 μSv/h. As mentioned in section 2.3, the air dose rate and soil moisture content were calculated using Eq. (1). The coefficient of determination (R^2) score between the observed value and moving average was 0.85 and 0.99 for the air dose rate and soil moisture content, respectively. The R^2 score for the soil moisture content was close to 1, indicating that there was little difference between the observed values and moving average.

NaI (Tl) scintillation survey meters results were 4.62 μSv/h on June 10, 2021 and 4.45 μSv/h on July 12, 2021. In Namie-Town, the values are smaller than those of the D-Shuttle because the scintillation observations were made horizontally to the slope, while the D-Shuttle was installed vertically to the slope. When scintillation was measured horizontally and vertically to the slope, the results for the vertical direction tended to be higher, around 1.0 μSv/h maybe due to radiation from the soil.

3.2. Changes in soil moisture content and air dose rate

The air dose rate decreased as the soil moisture content increased and the R^2 score was 0.82 compared with that of the respective data. As soil moisture increased, airflow decreased, with a correlation coefficient of −0.91. The air dose rate can be estimated as shown in Eq. (4).

$$z_{I(t)} = -0.179 y_{(t)} + 11.653 \quad (4)$$

The air dose rate at time t is denoted by $z_{(t)}$ [μSv/h] and the soil moisture at time t content by $y_{(t)}$ [%]. Note that in Eq (4) can be adapted for $20 < y_{(t)} < 50$. The reason for this is that the soil moisture content never fell below 20% and never exceeded 50% between May and October of 2021. The observed values of the air dose rates and estimated value (I) calculated using Eq. (4) are shown in Fig. 2(a). The estimated value (I) can be used to estimate a rough temporal change in the observed value. In other words, the decrease in air dose rate in this area is attributed to a rainfall-related increase in soil moisture content in most cases. In addition, the period during which the air dose rates increased coincided with the period during which the soil moisture content decreased, indicating that soil moisture conditions affected long-term changes in air dose rates over several days.

In the forests of Namie-Town, the shielding effect of soil moisture on radioactive materials released from the soil is greater than the fallout effect during rainfall and the impact of 99% of the total soil inventory of

Table 1
Results for the observation period.

	Count [h]	Rainfall [mm]				Soil moisture content [%]				Air dose rate [μSv/h]			
		sum	Max	min	median	standard deviation	average	max	min	median	standard deviation	average	max	min	median	standard deviation
Namie-Town	1687	313	17.5	0	0	0.973	31.1	36.5	28.9	30.9	1.295	6.08	6.87	5.23	6.07	0.275
Kawauchi-Village	1489	403	13.5	0	0	1.083	18.1	30.5	10.5	18.7	4.973	0.29	0.46	0.16	0.29	0.036

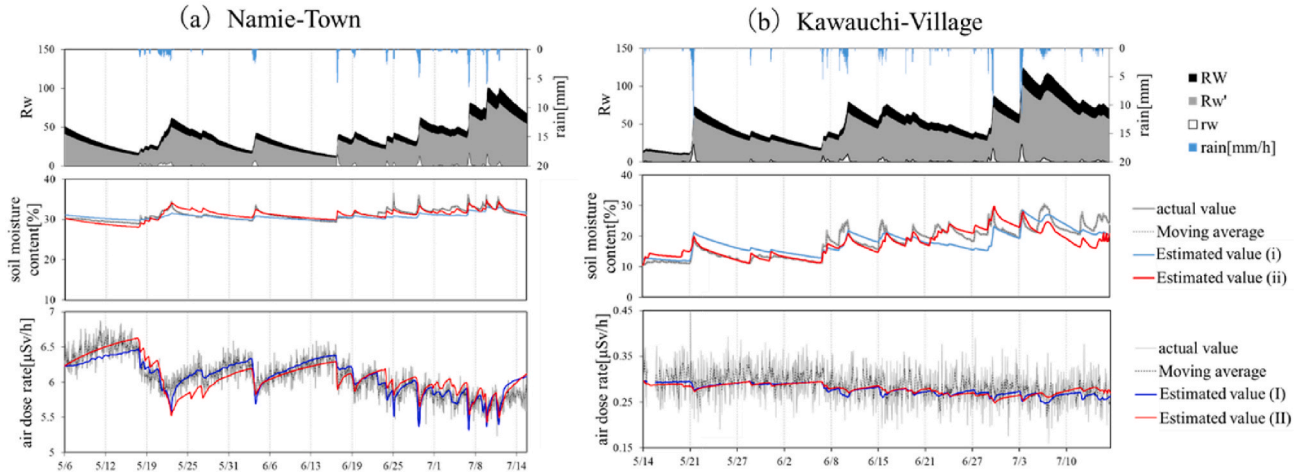

Fig. 2. Change in rainfall and effective rainfall, soil moisture content, and air dose rate (from top to bottom).

Fukushima-derived ^{137}Cs in the upper 10 cm of typical conifer forest soil (Teramage et al., 2014). Furthermore, changes in soil moisture conditions have a notable effect on ambient dose rates, not only when the soil is wet but also when the soil surface layer is dry. Therefore, the air dose rates are higher when the soil surface layer is dry.

3.3. Estimation of optimal half-life

Using Eq. (2), we compared the relationship between soil moisture content and air dose rate using various half-lives. The results showed that rainfall events with a short half-life of a few hours (short-term *Rw*) correlated well with the soil moisture content, while rainfall events with a long half-life of a few days (long-term *Rw*) also correlated well with soil moisture content. Therefore, it is insufficient to limit the half-life to one. Here, *Rw* was calculated by combining half-lives of several hours and days and comparing the *Rw* with the soil moisture content. A previous study (Nakai et al., 2006) have used long-term *Rw* and short-term *Rw* as an indicator of the effect of preceding rainfall and rainfall intensity immediately before the rainfall, respectively. Thus, we hypothesized that *Rw* combined with various half-lives would be sufficient. The subsequent results showed that short-term *Rw; rw* with a half-life of 2 h and long-term *Rw; RW* with a half-life of 7 days were adequate to obtain good results. Furthermore, the best correlation with soil moisture content was obtained when the new effective rainfall (*Rw'*) was calculated using *rw* of 20% and *RW* of 80%. Thus, *Rw'* was calculated as shown in Eq. (5):

$$Rw' = rw \times 0.20 + RW \times 0.80. \quad (5)$$

The soil moisture content increased and the air dose rate decreased as *Rw'* increased (Fig. 2(a)). During the observation period, *Rw'* and soil moisture content were positively (0.75) and negatively (−0.72) correlated with the air dose rate, respectively.

3.4. Relationship between effective rainfall and soil moisture content

The soil moisture content at the time *t* from *Rw'* can be estimated using Eq. (6):

$$y_{i(t)} = 0.0595 Rw'_{(t)} + 29.136. \quad (6)$$

The *rw* value increased with the onset of rainfall, and *rw* increased rapidly when the rainfall intensity increased. Furthermore, the *rw* value reached zero a few hours after rainfall ceased. In contrast, although the *RW* value never reached 0, it showed a gradual decreasing trend. The combination of *Rw* with different half-lives indicates that the moisture content in the soil does not decay with a constant half-life. The short half-life and fast decay rate of the short-term *Rw* indicates that the water flow percolates downward and is not stored in the soil surface layer. The slow decay rate of the long-term *Rw* suggests the presence of water that has been stored in the soil for a long time. Since the long-term *Rw* accounts for most of the water in the soil, it might indicate that most of the water in the soil has been stored for several days.

The estimated change (i) in soil moisture content over time, which was calculated using Eq. (6) is shown in Fig. 2(a). Although the timing of the increase in soil moisture content was captured, the estimated value (i) underestimated the observed soil moisture content value. Nonetheless, the estimation of soil moisture content during the drainage process, during which the soil moisture content decreases, seemed to be successful, and the relationship between effective rainfall and soil moisture content in one rainfall event (Fig. 3) indicates that the soil moisture content values were different during the increased and decreased periods of effective rainfall. Thus, hysteresis existed in the relationship between effective rainfall and soil moisture content, resulting in differences between the water absorption and drainage processes. This explains why the estimated value (i) could be successfully estimated for the drainage process, whereas it could not be successfully estimated for the water absorption process. Therefore, it is necessary to distinguish between water absorption and drainage processes to enable a more sophisticated estimation of the observed values for both processes. We used the effective rainfall $Rw'_{(t)}$ at time *t* and the effective rainfall $Rw'_{(t)}$ at time *t-1*, 1 h before time *t*. $Rw'_{(t-1)} < Rw'_{(t)}$ was considered to be the water absorption process, and $Rw'_{(t-1)} > Rw'_{(t)}$ was considered to be the

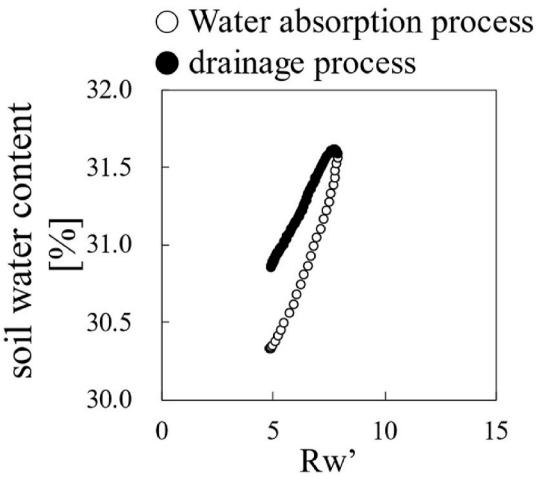

Fig. 3. Scatter plot of soil moisture content and air dose rate for the rain event.

drainage process. To express the difference between the water absorption and drainage processes, the change in soil moisture content with respect to the change in effective rainfall was defined as α.

$$\alpha = \pm \textit{ soil water content}/\pm \textit{ effective rainfall} = y_{(t)} - y_{(t-1)} \Big/ Rw'_{(t)} - Rw'_{(t-1)} \quad (7)$$

By transforming Eq. (7), Eq. (8) can be expressed as follows.

$$y_{(t)} = \alpha\left(Rw'_{(t)} - Rw'_{(t-1)}\right) + y_{(t-1)} \quad (8)$$

Once α is determined, the soil moisture content at time t can be estimated from the effective rainfall at time t and time t-*1* and the soil moisture content at time t-*1*.

Although α was the same in the drainage process for many rainfall events, it was different in the water absorption process. The amount of change of *Rw'* ($\pm Rw'$) for each rainfall event was the main reason for this difference in α for the water absorption process. The change in α for each rainfall event is shown in Fig. 4(a), with α on the vertical axis and $\pm Rw'$ on the horizontal axis; α was large when $\pm Rw'$ was small and decreased as $\pm Rw'$ increased. The water absorption process α at this time can be expressed by Eq. (9):

$$\alpha = 0.5417 \times \left(\pm Rw'^{-0.554}\right). \quad (9)$$

The R^2 score for this power approximation was 0.86, indicating a relationship between rainfall, $\pm Rw'$, and α. Rainfall intensity was also compared with α, but the relationship was not as strong as that for rainfall. The change in soil moisture content with respect to the change in effective rainfall is a critical reason as to why α decreases with increasing rainfall, $\pm Rw'$. A higher $\pm Rw'$ value indicates a greater increase in effective rainfall. However, the moisture content of the soil did not increase as the soil approached saturation, and the rate of the increase in soil moisture content decreased relative to the rate of the increase in effective rainfall; consequently, α decreased.

In the drainage process, α was similar for most rainfall events, but α was smaller when more time elapsed since the rainfall than α immediately after the rainfall. Therefore, we set α to 0.24, immediately after rainfall and to 0.08, 24 h after rainfall. Because the coarse pore spaces are less likely to retain water than fine pore spaces in the drainage process, the value of α was larger immediately after rainfall. In contrast, the value of α decreased with time because water drained from the fine pore spaces.

3.5. Estimation of soil moisture content and air dose rate in Namie-Town

To estimate the soil moisture content from effective rainfall, the estimation must be separated into the water absorption process (Eq. (10)), drainage process immediately after rainfall (Eq. (11)), and drainage process 24 h after rainfall (Eq. (12)).

$$y_{ii(t)} = 0.5417 \times \left(\pm Rw'^{-0.554}\right)\left(Rw'_{(t)} - Rw'_{(t-1)}\right) + y_{ii(t-1)} \quad (10)$$

$$y_{ii(t)} = 0.24\left(Rw'_{(t)} - Rw'_{(t-1)}\right) + y_{ii(t-1)} \quad (11)$$

$$y_{ii(t)} = 0.08\left(Rw'_{(t)} - Rw'_{(t-1)}\right) + y_{ii(t-1)} \quad (12)$$

This estimation can be performed by using the initial soil moisture content. Using Eq. (10)–(12), the estimated value (ii) of the soil moisture content was determined (Fig. 2(a)). The correlation value between the moving average and estimated values (ii) of the soil moisture content exceeded 0.85.

Next, the soil moisture content estimated from the effective rainfall was used to estimate the air dose rate by substituting into Eq. (4). The correlation score between the moving average and estimated values (ii) was 0.84. The estimated value (ii) of the air dose rate (Fig. 2(a)) was sufficiently estimated for the observed values. In some cases, the estimated values were under- or overestimated. These deviations occur in the estimation of soil moisture content from effective rainfall. Thus, if the soil moisture content can be correctly estimated from the effective rainfall, the air dose rate can also be estimated with a small error. In conclusion, it is possible to estimate the soil moisture content and air dose rate from the effective rainfall, and the correlation values for both exceeded 0.80.

4. Testing of estimation method in Kawauchi-Village, Futaba-gun, Fukushima

We tested whether the same estimation method could be applied to Kawauchi-Village. The air dose rates in Kawauchi-Village are more than one order of magnitude lower than those in Namie-Town because of defoliation and clearcutting. Therefore, we tested whether air dose rates could be estimated from changes in soil moisture content, even in areas with low air dose rates. NaI (Tl) scintillation survey meters results were 0.38 μSv/h on May 17, 2019 and 0.34 μSv/h on June 14, 2019. The correlations between the measured value and moving average were 0.56 and 0.99 for air dose rates and soil moisture content, respectively. The correlation between the moving average of soil moisture content and the air dose rate was 0.64, which can be expressed by Eq. (13):

$$z_{(t)} = -0.0025 y_{(t)} + 0.3327 \quad (13)$$

Eq (13) can be adapted for $10 < y_{(t)} < 50$. Fig. 2(b) shows these changes over time. In Kawauchi-Village, in addition to the effects of changes in air dose rates due to rainfall-related changes in soil moisture content, decreases and increases in air dose rates occur at times other than during rainfall.

Next, we attempted to estimate the soil moisture content from the effective rainfall. We examined the relationship between $\pm Rw'$. and α

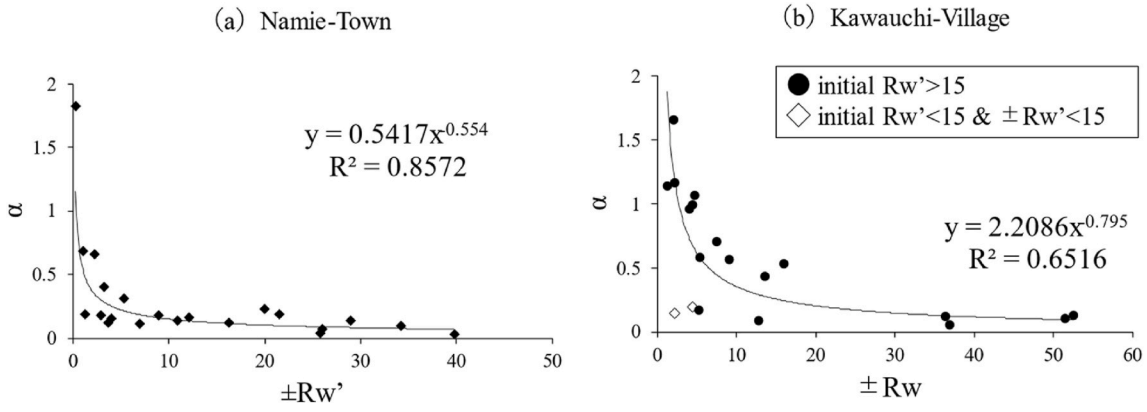

Fig. 4. Diagram of $\pm Rw$ and the change in soil moisture content concerning the change in effective rainfall (α).

for each rainfall event and found that for single rainfall events with $\pm Rw'$ of 15 or less, there were rainfall events in which α became a power-law approximation with increasing integrated rainfall, as in Namie-Town, and rainfall events in which α became very small (Fig. 4 (b)). The rainfall events with an extremely small α were those with $\pm Rw'$ of 15 or less and an initial $\pm Rw'$ of $\leq$15 before the rainfall event. We considered this factor to contribute to the water repellency of the soil and measured the water repellency of the soil in Kawauchi-Village. Results are shown in the Supplementary Fig. 2. The investigation method is shown in Section 2.5. The water repellency of the soil samples increased with increasing soil moisture content and disappeared at a certain value. In Kawauchi-Village, the highest water repellency occurred in samples with a soil moisture content of 15%. In Kawauchi-Village, the critical moisture content, which was defined as the soil moisture content at which the water repellency disappeared, was 30%, and the soil moisture content during the observation period ranged from 10.5 to 30.5%, which is within the range at which water repellency could occur. However, the water repellency did not disappear owing to insufficient rainfall, because the soil moisture content was less than 15% and the accumulated rainfall was less than 10 mm. Therefore, although the rainfall events increased the effective rainfall, the infiltration of water into the soil was intercepted and the soil moisture content hardly increased, leading to rainfall events with a very small α. Although the air dose rates increased and decreased in some cases, the changes were slight and within the margin of error.

In Namie-Town, the critical moisture content and maximum water repellency was 20% and 10%, respectively.

In Kawauchi-Village, as in Namie-Town, soil moisture content was estimated from *Rw*, resulting in α as shown in Table 2. The correlation at this time is 0.84. Time series changes are shown in Fig. 2(b). Water repellency appeared on May 14 and May 20, and even though the moving average of soil moisture content did not increase at these times, the estimate value increased significantly. Therefore, further study is needed for estimation in soils where water repellency is present. The air dose rate was estimated from the soil moisture content obtained from *Rw* using Eq. (13). The correlation coefficient between the moving average and the estimate value from *Rw'* was −0.57, which was not significantly different from the estimate value from soil moisture content.

5. Discussion

The results of this study confirmed that changes in the soil moisture content are a key factor influencing changes in the air dose rates. In other words, even within the same forest, the air dose rates differed depending on the soil surface conditions at each site. Moreover, since the presence or absence of water repellency affects the estimation of soil moisture content and air dose rate, the presence of radiation sources and water repellency at the ground surface should be evaluated in future studies.

^{137}Cs inventory in soil 0–10 cm and litter is 2845 kBq/m^2 (March 29, 2019) in Namie-Town and 183 kBq/m^2 (November 27, 2019) in Kawauchi-Village. The vertical distribution of ^{137}Cs inventory is shown in the Supplemental Fig. 4. The deposition density of ^{137}Cs in soil in Kawauchi-Village is smaller than that in Namie-Town because of the removal of debris and clear cutting in the past. High radiation levels are detected within 5 cm from the soil surface (Malins et al., 2021). However, we believe that in Kawauchi-Village, where the ^{137}Cs concentration in the surface layer is small, the radiation dose shielding effect of increased soil moisture was not significant. Sufficient ^{137}Cs in the soil would be required for the estimates of this study to be applicable. Therefore, it is necessary to focus on the effect of initial deposition density of ^{137}Cs in soil in the future.

In this study, only summer data from May to July 2019 were used. However, as changes in soil moisture content differ between summer and winter due to changes in solar radiation and temperature (Tamai, 2017), observations throughout the year are needed to estimate the general air dose rates in the future. It is possible to estimate the extent of the impact of rainfall during the onset of summer rainfall by estimating historical data in a similar manner. When this method is used to estimate historical air dose rates, it can be assumed that the amount of radiation from the ground surface is immense; thus, the amount of radiation intercepted when the soil moisture content increases can also be estimated to be significant. Therefore, the coefficients used in Eq. (13) and obtained as of 2019 in this analysis, may need to be changed.

This study estimated the rainfall-associated decrease in air dose rate. Conversely, this method makes it possible to estimate, to some extent, the presence of rainfall and changes in soil moisture content from changes in the air dose rate. Thus, the period in which the air dose rate temporarily decreased can be considered as the period during which rainfall occurred and the soil moisture content increased. If the equations calculated in this study can be used successfully, there is a high possibility that this method can be used to estimate the soil moisture content using an air dose-monitoring network.

Table 2
Value of α

	Water absorption process	Drainage process	
		Immediately	24 h after
Namie-Town	$(\pm Rw') \times 0.5417^{-0.554}$	0.23	0.08
Kawauchi-Village	$(\pm Rw') \times 2.2086^{-0.795}$	0.45	0.20

6. Conclusion

By focusing on the shielding effect of water, we estimated the changes in air dose rates using observed changes in soil moisture content for two forests in the Fukushima Prefecture. We estimated soil moisture content using effective rainfall calculated from JMA rainfall data, and then estimated air dose rates. However, in areas such as Kawauchi-Village, where air dose rates are low, it was difficult to capture changes in air dose rates due to changes in soil moisture content. In this study, we were able to estimate soil moisture content and air dose rate from rainfall in high dose areas and were able to capture the effect of rainfall on the decreasing trend of air dose rate. Therefore, this study can be used as an indicator to determine whether temporary changes in air dose rates are caused by influences other than rainfall. The results of this study could also contribute to the improvement of current methods that estimate the external dose rates for humans, terrestrial animals, and forest plants.

Funding

This work was supported by the Grant-in-Aid for Scientific Research on Innovative Areas [grant number 24110005]; Grant-in-Aid for Scientific Research (A) [grant number 22H00556]; Agence Nationale de la Recherche [grant number [ANR-11-RSNR-0002]; and the Japan Science and Technology Agency, as part of the Belmont Forum.

Credit author statement

Miyu Nakanishi; Investigation, Methodology, Writing – original draft. **Yuichi Onda**; Writing – review & editing. **Hiroaki Kato**, Investigation. **Junko Takahashi**; Investigation. **Hikaru Iida**; Investigation, Methodology. **Momo Takada**; Methodology.

Declaration of competing interest

The authors declare the following financial interests/personal relationships which may be considered as potential competing interests: Yuichi Onda reports financial support was provided by University of Tsukuba.

Data availability

The data that has been used is confidential.

Acknowledgments

We would like to acknowledge the Study on the verification and development of technological measures to control radioactive materials in forests project of the Ministry of Agriculture, Forestry and Fisheries, for data collection.

Appendix A. Supplementary data

Supplementary data to this article can be found online at https://doi.org/10.1016/j.envpol.2023.122147.

References

Adachi, N., Adamovitch, V., Adjovi, Y., Aida, K., Akamatsu, H., Akiyama, S., Akli, A., Ando, A., Andrault, T., Antonietti, H., 2016. Measurement and comparison of individual external doses of high-school students living in Japan, France, Poland and Belarus—the 'D-shuttle' project. J. Radiol. Prot. 36, 49–66. https://doi.org/10.1088/0952-4746/36/1/49.

Basuki, T., Bekelesi, W.C., Tsujimoto, M., Nakashima, S., 2020. Air dose rate to 137Cs activity per unit area ratio for different land use 7 years after the nuclear accident -Case of the slope catchment, Ogi reservoir, Fukushima. Radiat. Meas. 137 https://doi.org/10.1016/j.radmeas.2020.106424.

Cammeraat, L.H., Imeson, A.C., 1999. The evolution and significance of soil-vegetation patterns following land abandonment and fire in Spain. Catena 37 (1–2), 107–127. https://doi.org/10.1016/S0341-8162(98)00072-1.

Fukuda, T., Yokota, S., Iwamatsu, A., Wada, T., 2009. Infiltration process of rainwater into soft ignimbrite slopes and the prediction of the occurrence of slope failures. J. Japan Soc. Eng. Geol. 50 (4), 216–227. https://doi.org/10.5110/jjseg.50.216 (in Japanese).

Imamura, N., Akama, A., Ohtani, Y., Kobayashi, M., Tsuboyama, Y., Takahashi, M., 2017. An estimation of air dose rate from considering of radiocesium distribution in Japanese forests. J. Jpn. For. Soc. 99 (1), 1–9. https://doi.org/10.4005/jjfs.99.1 (in Japanese).

Kato, H., Onda, Y., Wakahara, T., Kawamori, A., 2018. Spatial pattern of atmospherically deposited radiocesium on the forest floor in the early phase of the Fukushima Daiichi Nuclear Power Plant accident. Sci. Total Environ. 615, 187–196. https://doi.org/10.1016/j.scitotenv.2017.09.212.

Kawano, T., Tsuruta, R., Yoshimoto, T., Uchida, K., 2019. Comparison of poparty of electronic dosimeter "D-shuttle" and air dose rate measuring devices. Res. Rep. From Ishikawa Prefectural Institute Of Public Health And Environ. Sci. 57, 74–75 (in Japanese).

Keizer, J.J., Doerr, S.H., Malvar, M.C., Prats, S.A., Ferreira, R.S.V., Oñate, M.G., Coelho, C.O.A., Ferreira, A.J.D., 2008. Temporal variation in topsoil water repellency in two recently burnt eucalypt stands in north-central Portugal. Catena 74 (3), 192–204. https://doi.org/10.1016/j.catena.2008.01.004.

Kobayashi, M., 2013. Water repellency of forest soils. J. Hydraulic Sci. 57 (2), 13–35. https://doi.org/10.20820/suirikagaku.57.2_13 (in Japanese).

Lozano, E., Jiménez-Pinilla, P., Mataix-Solera, J., Arcenegui, V., Bárcenas, G.M., González-Pérez, J.A., García-Orenes, F., Torres, M.P., Mataix-Beneyto, J., 2013. Biological and chemical factors controlling the patchy distribution of soil water repellency among plant species in a Mediterranean semiarid forest. Geoderma 207–208 (1), 212–220. https://doi.org/10.1016/j.geoderma.2013.05.021.

Malins, A., Imamura, N., Niizato, T., Takahashi, J., Kim, M., Sakuma, K., Shinomiya, Y., Miura, S., Machida, M., 2021. Calculations for ambient dose equivalent rates in nine forests in eastern Japan from 134Cs and 137Cs radioactivity measurements. J. Environ. Radioact. 226 https://doi.org/10.1016/j.jenvrad.2020.106456.

Minato, S., 1980. Analysis of time variations in natural background gamma radiation flux density. J. Nucl. Sci. Technol. 17 (6), 461–469. https://doi.org/10.3327/jnst.17.461.

Mirbabaei, S.M., Shabanpour, M., van Dam, J., Ritsema, C., Zolfaghari, A., Khaledian, M., 2021. Observation and simulation of water movement and runoff in a coarse texture water repellent soil. Catena 207. https://doi.org/10.1016/j.catena.2021.105637.

Nagaoka, T., Sakamoto, R., Saito, K., Tsutsumi, M., Moriuchi, S., 1988. Diminution of terrestrial gamma ray exposure rate due to snow cover. Japanese J. Health Phys. 23 (4), 309–315. https://doi.org/10.5453/jhps.23.309 (in Japanese).

Nakai, S., Sasaki, Y., Kaibori, M., Moriwaki, T., 2006. Rainfall index for warning and evacuation against sediment-related disaster: reexamination of rainfall index Rf, and proposal of R. Soils Found. 46 (4), 465–475. https://doi.org/10.3208/sandf.46.465.

Nelson, M.S., Rittenour, T.M., 2015. Using grain-size characteristics to model soil water content: application to dose-rate calculation for luminescence dating. Radiat. Meas. 81, 142–149. https://doi.org/10.1016/j.radmeas.2015.02.016.

Onda, Y., Taniguchi, K., Yoshimura, K., Kato, H., Takahashi, J., Wakiyama, Y., Coppin, F., Smith, H., 2020. Radionuclides from the fukushima daiichi nuclear power plant in terrestrial systems. Nat. Rev. Earth Environ. 1 (12), 644–660. https://doi.org/10.1038/s43017-020-0099-x.

Sanada, Y., Yoshimura, K., Urabe, Y., Iwai, T., Katengeza, E.W., 2020. Distribution map of natural gamma-ray dose rates for studies of the additional exposure dose after the Fukushima Dai-ichi Nuclear Power Station accident. J. Environ. Radioact. 223, 224. https://doi.org/10.1016/j.jenvrad.2020.106397.

Schimmack, W., Steindl, H., Bunzl, K., 1998. Variability of water content and of depth profiles of global fallout 137Cs in grassland soils and the resulting external gamma-dose rates. Radiat. Environ. Biophys. 37, 27–33.

Seaton, F.M., Jones, D.L., Creer, S., George, P.B.L., Smart, S.M., Lebron, I., Barrett, G., Emmett, B.A., Robinson, D.A., 2019. Plant and soil communities are associated with the response of soil water repellency to environmental stress. Sci. Total Environ. 687, 929–938. https://doi.org/10.1016/j.scitotenv.2019.06.052.

Shimamura, M., 2003. Verification of the effectiveness of rainfall warning using effective rainfall. Technical Review, JR East 3, 45–48 (in Japanese).

Smettem, K.R.J., Rye, C., Henry, D.J., Sochacki, S.J., Harper, R.J., 2021. Soil water repellency and the five spheres of influence: a review of mechanisms, measurement and ecological implications. In: Science of the Total Environment, vol. 787. Elsevier B.V. https://doi.org/10.1016/j.scitotenv.2021.147429.

Tamai, K., 2017. Characteristics and factors relating to seasonal fluctuation of evaporation from forest floor - observations in Japanese and Cambodian forests. Water Sci. 61 (5), 1–21. https://doi.org/10.20820/suirikagaku.61.5_1 (in Japanese).

Teramage, M.T., Onda, Y., Kato, H., Gomi, T., 2014. The role of litterfall in transferring Fukushima-derived radiocesium to a coniferous forest floor. Sci. Total Environ. 490, 435–439. https://doi.org/10.1016/j.scitotenv.2014.05.034.

Tsuchida, D., Yaguchi, R., Yamazawa, H., Narazaki, Y., 2020. Meteorological mechanism of a high dose rate event caused by the eastward advance of a low pressure system during rainy season. Japanese J. Health Phys. 55 (1), 5–14. https://doi.org/10.5453/JHPS.55.5 (in Japanese).

Urbanek, E., Walsh, R.P.D., Shakesby, R.A., 2015. Patterns of soil water repellency change with wetting and drying: the influence of cracks, roots and drainage conditions. Hydrol. Process. 29 (12), 2799–2813. https://doi.org/10.1002/hyp.10404.